

AD-A277 007 ATION PAGE

Form Approved  
OMB No. 0704-0188

2



On average 1 hour per response, including the time for reviewing instructions, searching existing data sources, gathering the collection of information. Send comments regarding this burden estimate or any other aspect of this collection of information, including suggestions for reducing this burden, to Washington Headquarters Services, Directorate for Information Operations and Reports, 1215 Jefferson Avenue, Washington, DC 20540-6001, and to the Office of Management and Budget, Paperwork Reduction Project (0704-0188), Washington, DC 20503.

1. AGENCY USE ONLY (Leave blank)		2. REPORT DATE February 1994	3. REPORT TYPE AND DATES COVERED Interim
4. TITLE AND SUBTITLE Electrostrictive ceramics for underwater transducer applications.			5. FUNDING NUMBERS PE - 61153N TA - RR011-08-42 WU - DN 580-030
6. AUTHOR(S) Kurt M. Rittenmyer			
7. PERFORMING ORGANIZATION NAME(S) AND ADDRESS(ES) Naval Research Laboratory Underwater Sound Reference Detachment PO Box 568337 Orlando, FL 32856-8337			8. PERFORMING ORGANIZATION REPORT NUMBER  N/A
9. SPONSORING/MONITORING AGENCY NAME(S) AND ADDRESS(ES) Naval Research Laboratory Washington, DC 20375-5000			10. SPONSORING/MONITORING AGENCY REPORT NUMBER  N/A
11. SUPPLEMENTARY NOTES  Published in J. Acoust. Soc. Am. 95(2), Feb. 1994			
12a. DISTRIBUTION/AVAILABILITY STATEMENT  Approved for public release; distribution unlimited.			12b. DISTRIBUTION CODE
13. ABSTRACT (Maximum 200 words)  The electromechanical properties of two electrostrictive materials designed for use in underwater acoustic applications are determined as functions of temperature and electric field. The materials are $0.859\text{Pb}(\text{Mg}_{1/3}\text{Nb}_{2/3})\text{O}_3$ - $0.141\text{PbTiO}_3$ doped with 2.5% $\text{SrTiO}_3$ or $\text{BaTiO}_3$ . Dielectric properties are determined as functions of temperature and electric field. The equivalent piezoelectric coefficients were found as functions of temperature to be equal to or superior to the lead zirconate-titanate ceramics at very modest dc bias fields (2 kV/cm) at temperatures in the range from 10 at 35°C. Outside of this temperature range, the piezoelectric and dielectric coefficients decrease rapidly. Electromechanical losses were found to be sufficiently small for the $\text{SrTiO}_3$ composition but not the $\text{BaTiO}_3$ composition.			
14. SUBJECT TERMS Electrostrictive ceramics Lead magnesium niobate Acoustic transducers			15. NUMBER OF PAGES 8
			16. PRICE CODE
17. SECURITY CLASSIFICATION OF REPORT UNCLASSIFIED	18. SECURITY CLASSIFICATION OF THIS PAGE UNCLASSIFIED	19. SECURITY CLASSIFICATION OF ABSTRACT UNCLASSIFIED	20. LIMITATION OF ABSTRACT UL

## GENERAL INSTRUCTIONS FOR COMPLETING SF 298

The Report Documentation Page (RDP) is used in announcing and cataloging reports. It is important that this information be consistent with the rest of the report, particularly the cover and title page. Instructions for filling in each block of the form follow. It is important to **stay within the lines** to meet **optical scanning requirements**.

**Block 1. Agency Use Only (Leave blank).**

**Block 2. Report Date.** Full publication date including day, month, and year, if available (e.g. 1 Jan 88). Must cite at least the year.

**Block 3. Type of Report and Dates Covered.** State whether report is interim, final, etc. If applicable, enter inclusive report dates (e.g. 10 Jun 87 - 30 Jun 88).

**Block 4. Title and Subtitle.** A title is taken from the part of the report that provides the most meaningful and complete information. When a report is prepared in more than one volume, repeat the primary title, add volume number, and include subtitle for the specific volume. On classified documents enter the title classification in parentheses.

**Block 5. Funding Numbers.** To include contract and grant numbers; may include program element number(s), project number(s), task number(s), and work unit number(s). Use the following labels:

<b>C</b> - Contract	<b>PR</b> - Project
<b>G</b> - Grant	<b>TA</b> - Task
<b>PE</b> - Program Element	<b>WU</b> - Work Unit Accession No.

**Block 6. Author(s).** Name(s) of person(s) responsible for writing the report, performing the research, or credited with the content of the report. If editor or compiler, this should follow the name(s).

**Block 7. Performing Organization Name(s) and Address(es).** Self-explanatory.

**Block 8. Performing Organization Report Number.** Enter the unique alphanumeric report number(s) assigned by the organization performing the report.

**Block 9. Sponsoring/Monitoring Agency Name(s) and Address(es).** Self-explanatory.

**Block 10. Sponsoring/Monitoring Agency Report Number.** (If known)

**Block 11. Supplementary Notes** Enter information not included elsewhere such as: Prepared in cooperation with...; Trans. of...; To be published in... When a report is revised, include a statement whether the new report supersedes or supplements the earlier report.

**Block 12a. Distribution/Availability Statement.** Denotes public availability or limitations. Cite any availability to the public. Enter additional limitations or special markings in all capitals (e.g. NOFORN, REL, ITAR).

**DOD** - See DoDD 5230.24, "Distribution Statements on Technical Documents."

**DOE** - See authorities.

**NASA** - See Handbook NHB 2200.2.

**NTIS** - Leave blank.

**Block 12b. Distribution Code.**

**DOD** - Leave blank.

**DOE** - Enter DOE distribution categories from the Standard Distribution for Unclassified Scientific and Technical Reports.

**NASA** - Leave blank.

**NTIS** - Leave blank.

**Block 13. Abstract.** Include a brief (*Maximum 200 words*) factual summary of the most significant information contained in the report.

**Block 14. Subject Terms.** Keywords or phrases identifying major subjects in the report.

**Block 15. Number of Pages.** Enter the total number of pages.

**Block 16. Price Code.** Enter appropriate price code (*NTIS only*).

**Blocks 17. - 19. Security Classifications.** Self-explanatory. Enter U.S. Security Classification in accordance with U.S. Security Regulations (i.e., UNCLASSIFIED). If form contains classified information, stamp classification on the top and bottom of the page.

**Block 20. Limitation of Abstract.** This block must be completed to assign a limitation to the abstract. Enter either UL (unlimited) or SAR (same as report). An entry in this block is necessary if the abstract is to be limited. If blank, the abstract is assumed to be unlimited.

# Electrostrictive ceramics for underwater transducer applications

Kurt M. Rittenmyer

Naval Research Laboratory, Underwater Sound Reference Detachment, P.O. Box 568337, Orlando, Florida 32856-8337

(Received 6 July 1993; accepted for publication 2 November 1993)

The electromechanical properties of two electrostrictive materials designed for use in underwater acoustic applications are determined as functions of temperature and electric field. The materials are  $0.859 \text{ Pb}(\text{Mg}_{1/3}\text{Nb}_{2/3})\text{O}_3$ – $0.141 \text{ PbTiO}_3$  doped with 2.5%  $\text{SrTiO}_3$  or  $\text{BaTiO}_3$ . Dielectric properties are determined as functions of temperature and electric field. The equivalent piezoelectric coefficients were found as functions of temperature to be equal to or superior to the lead zirconate–titanate ceramics at very modest dc bias fields (2 kV/cm) at temperatures in the range from 10 to 35 °C. Outside of this temperature range, the piezoelectric and dielectric coefficients decrease rapidly. Electromechanical losses were found to be sufficiently small for the  $\text{SrTiO}_3$  composition but not the  $\text{BaTiO}_3$  composition.

PACS numbers: 43.38.Ar, 43.38.Fx, 43.30.Yj

## INTRODUCTION

Lead magnesium niobate (PMN) and lead magnesium niobate–lead titanate (PMNPT) ceramics are capable of generating large strains at moderate electric field levels. Strains that are roughly an order of magnitude larger than those of the lead zirconate–lead titanate (PZT) ceramics can be achieved at high electric fields. This is due to the large dielectric permittivities of these materials which are also several times larger than those of the PZT materials. Such large dielectric permittivities are possible in the region of the ferroelectric–paraelectric phase transition. This is an order–disorder transformation. For PMNPT–ST, the transition covers a wide range (approximately 100 °C) of temperature.

The major focus of application for the electrostrictive relaxor materials has thus far been as actuators in optical systems.<sup>1,2</sup> In many cases, the temperature range of operation is narrow and fixed. For these applications, materials that can generate large strains with small thermal drifts are desired. PMN and PMNPT produce large strains while having thermal expansion coefficients that are a factor of 10 smaller than those of PZT. Because of their large effective strains, these materials represent a potential for substantial improvement in the performance of underwater transducer applications. However, most of these applications have different requirements than those of the optical actuators. These include applicability over a 0–30 °C temperature range, and small dielectric and mechanical losses at high ac-field levels (small hysteresis). The maximum obtainable strain is important but must be considered in light of these other requirements.

Relaxor ferroelectrics can be considered as a conglomerate of microscopic regions which are statistically distributed in composition. In particular, the two B-site cations (Mg and Nb in the materials discussed here) are ordered at low temperatures, but become increasingly disordered as the temperature is increased. At high temperatures, the distribution is completely random. The change in the distribution of cations causes a distribution of the Curie tem-

peratures thereby broadening the transition region of the material.<sup>3,4</sup>

Somewhat above their Curie temperature, relaxor ferroelectric materials are electrostrictive in nature, and therefore, do not maintain large remanent polarizations after the field is removed. Here, it is possible to control the effective piezoelectric coefficients by changing the bias field.<sup>4</sup> This has two important ramifications. First, unlike standard piezoceramics, the material will not be susceptible to permanent depoling under large stresses or mechanical shock. Also, removal of the bias field and discharging of the ceramic eliminates the effective direct piezoelectric effect (charge produced by applied stress). Consequently, the material will radiate or generate acoustic waves following mechanical shock or insonification once it is discharged to a much smaller extent compared with conventional poled piezoelectric ceramics.

While the fundamental electromechanical properties of PMNPT ceramics are outstanding, there are several problems which must be addressed before they can be widely applied in transducer designs. First, the nature of the order–disorder phase transition in relaxor ferroelectrics such as PMNPT dictates that both dielectric and piezoelectric properties will vary continuously but rather slowly over a wide range of temperature.<sup>3–5</sup> Also, the properties of the material will vary with frequency but in a much less dramatic fashion than with temperature. Second, the material is mechanically brittle and tends to develop cracks while cycling under high ac-electric fields. The latter problem can probably be addressed by slight compositional additives and improvements in processing methods. The first problem can be reduced by temperature stabilization of the ceramic and adjusting the maximum in the strong-field properties to be in the middle of the operating temperature range of interest (0–30 °C for most underwater transducers). This article describes the properties of two doped PMNPT materials which were developed for use in the temperature region of interest while maintaining the excellent electromechanical coupling of the material.

94-07756



94 3 9 008

## I. EXPERIMENT

### A. Sample preparation

Ceramics of two compositions, 0.975 (0.859 PMN-0.141 PT)-0.025 SrTiO<sub>3</sub>, labeled PMNPT-ST and 0.975 (0.859 PMN-0.141 PT)-0.025 BaTiO<sub>3</sub>, which is labeled PMNPT-BT were prepared by methods reported previously by Pilgrim *et al.*<sup>6</sup> In the following, these two compositions will be referred to as PMNPT-BT and PMNPT-ST, respectively. The best method for producing materials of high perovskite phase purity was described by Swartz and Shrout.<sup>7</sup> The method involves prereacting magnesium oxide and niobium oxide at 1100 °C and then grinding the resulting colombsite-structure material and mixing it with lead oxide and either SrCO<sub>3</sub> or BaCO<sub>3</sub> and TiO<sub>2</sub> and calcining the mixture at 800 °C for 3 h. This procedure lowers lead volatilization and promotes formation of the perovskite structure while inhibiting formation of an undesirable phase with the pyrochlore structure. The powder is then wet milled and sintered at 1200 °C to yield a dense ceramic with the perovskite crystal structure. It has superior dielectric and piezoelectric properties compared with other techniques. After dimensioning the samples by lapping and polishing, gold was applied onto the major parallel surfaces by sputtering. Silver ink electrodes were then fired on over the sputtered electrode. This procedure provides low resistivity electrodes so that the high dielectric permittivity of the material is not sacrificed by low permittivity interfacial layers. All samples were 4.3 mm thick.

### B. High-frequency measurements of the effective $d_{33}$ , $d_{31}$ , and $\epsilon_{33}^T$

A laser Doppler vibrometer (LDV)<sup>8</sup> was used to measure the strain in the electrostrictive ceramics as a function of frequency, temperature, and electric field. The procedure has been described in a previous article,<sup>9</sup> except the mounting of the sample was altered. A diagram of the system is shown in Fig. 1. The apparent  $d_{33}$  coefficients were determined by measuring the longitudinal strain of a rectangular sample (dimensions: 15×15×4.3 mm<sup>3</sup>). The precise geometry was prescribed by the application of the material in an actual underwater transducer. For measurements of  $d_{33}$ , the sample was attached at its center to a cylindrical wood rod with cyanoacrylate epoxy, and was subsequently fixed in an optical mount. Thin wire leads were used to connect the sample electrodes to a driving circuit shown in Fig. 2. For measurements of the  $d_{31}$  coefficient, the sample was mounted on edge with epoxy and the laser was focused on the opposite edge. A variable dc bias voltage is applied to the sample through a 2 MΩ resistor using a power supply<sup>10</sup> which is capable of supplying 0–10 kV dc. The power amplifier<sup>11</sup> outputs an audio signal (0.1–10 kHz) of magnitude from 0–20 V<sub>rms</sub>. This signal is then applied to the sample through a blocking capacitor (0.2 μF) which protects the output of the signal amplifier from the large dc voltage but allows the ac-signal to pass with minimal roll-off. The velocity amplitude of the vibrating surface is measured by the LDV system. The strain is

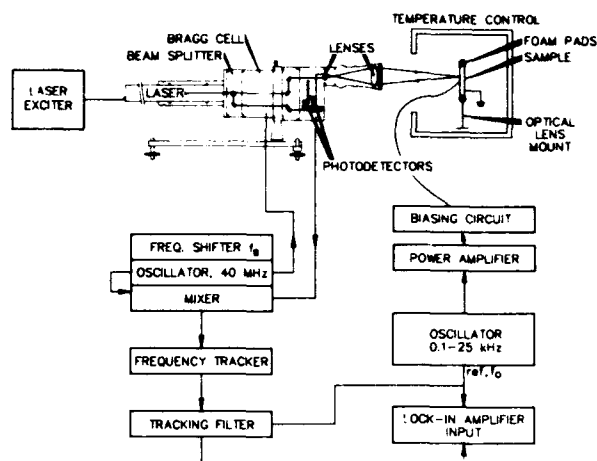


FIG. 1. Diagram of laser Doppler vibrometer and associated system used to directly measure piezoelectric coefficients.

calculated from the velocity of the surface. The appropriate piezoelectric coefficient ( $d_{33}$  or  $d_{31}$ ) is then calculated from the measured strain and ac electric field level. Bias fields of 1.0 and 2.0 kV/cm were utilized. Fields up to 7 kV/cm were obtainable by coating the edges of the samples with a dielectric silicone grease. However, dielectric breakdown around the edges of the sample prevented reliable measurements at electric fields greater than 3 kV/cm at most temperatures. Thinner samples would allow higher bias levels. Since the dimensions of the samples were dictated by their application in actual underwater transducers, their thickness was not varied.

The temperature dependence of the dielectric and piezoelectric properties of the materials was determined by placing the sample apparatus in a liquid-nitrogen-cooled environmental chamber<sup>12</sup> equipped with a window through which the laser can be focused. The unit can control temperature in the range from -70 to +315 °C but was used only in the range from -20 to 90 °C where the effective piezoelectric coefficients of the materials are sufficiently large. This is considerably larger than the intended range of application. The weak-field dielectric constant was monitored at each temperature and frequency using an impedance analyzer. By definition, the dielectric properties of relaxor ferroelectrics such as PMN and PMNPT are time dependent in the region of the phase transition from a

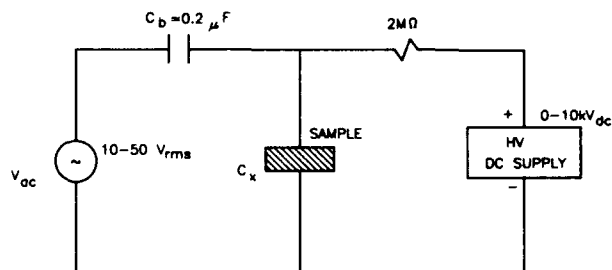


FIG. 2. Electrical circuit used to apply simultaneous ac and dc electric fields to a sample.

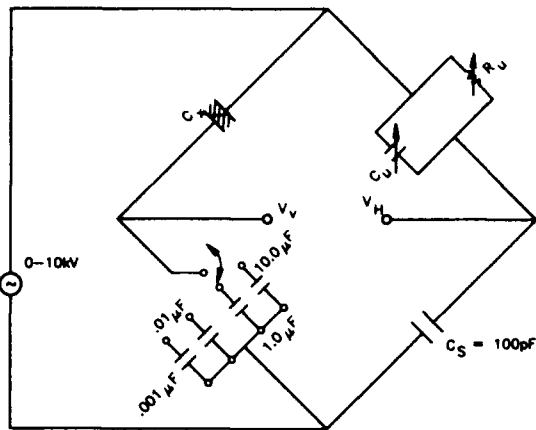


FIG. 3. Bridge circuit used to measure strong-field dielectric properties.

disordered nonpolar structure to an ordered polar structure. Consequently, the dielectric properties, at low fields, are highly dependent on the manner in which the sample is heated and cooled. Therefore, the measured value will depend on the heating rate and the amount of time the material is left to stabilize. In all tests, the temperature was allowed to equilibrate at each set temperature for about 15 min. At this point, the change in the properties was nearly negligible, although due to the aging characteristics<sup>13</sup> of the relaxor material in the microdomain-macrodomain region, the value obtained is always dependent on the time scale and frequency of the measurement. This procedure was followed for all of the measurements described here.

### C. Measurements of high-field dielectric and piezoelectric hysteresis as a function of temperature

The dielectric displacement and current of the two materials were measured as a function of electric field and temperature. A modified Sawyer-Tower circuit (Fig. 3) was used for high-field measurements. The electric field was varied from  $-10$  to  $+10$  kV/cm at low frequency

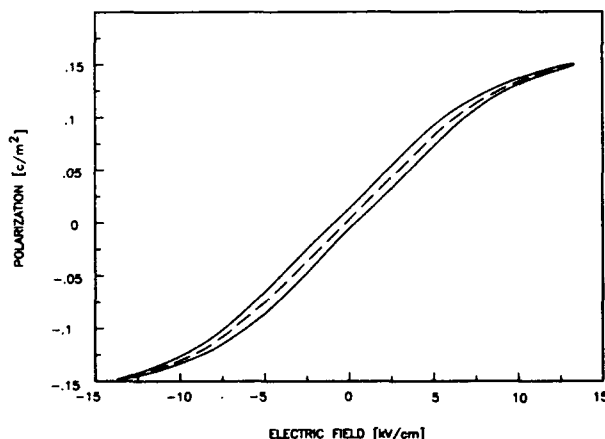


FIG. 4. Method of calculating dielectric permittivity from  $P$ - $E$  hysteresis as a function of electric field by averaging polarizations of increasing fields and decreasing fields at each value of electric field.

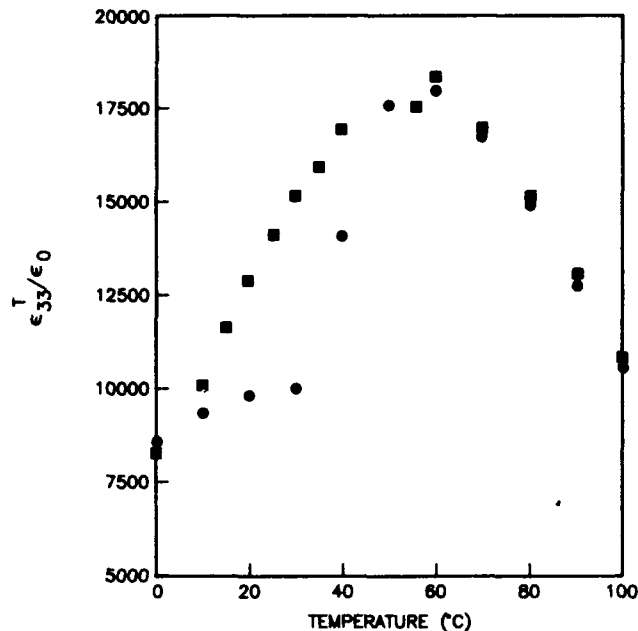


FIG. 5. Weak-field relative dielectric permittivity as a function of temperature for PMNPT-ST  $[0.975(0.859(\text{Pb}_3\text{MgNb}_2\text{O}_9) - 0.141(\text{PbTiO}_3)) - 0.025\text{SrTiO}_3]$ ; ● indicates increasing temperature, ■ indicates decreasing temperature.

( $0.05$ – $1$  Hz). The sample was immersed in a high dielectric fluid<sup>14</sup> to prevent dielectric breakdown around the sample edges. The outputs of the bridge were displayed on a digital oscilloscope from which the data could be entered into a computer. Typical  $P$ - $E$  hysteresis loop is shown in

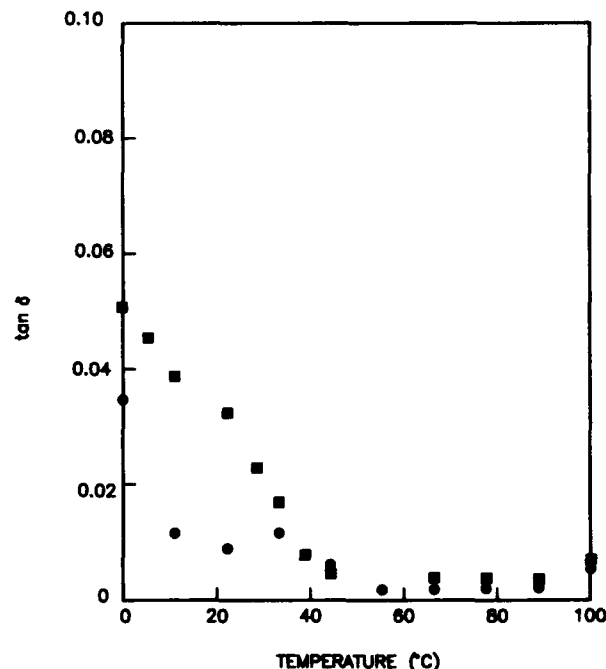


FIG. 6. Dielectric loss tangent as a function of temperature for PMNPT-ST  $[0.975(0.859(\text{Pb}_3\text{MgNb}_2\text{O}_9) - 0.141(\text{PbTiO}_3)) - 0.025\text{SrTiO}_3]$ ; ● indicates increasing temperature, ■ indicates decreasing temperature.

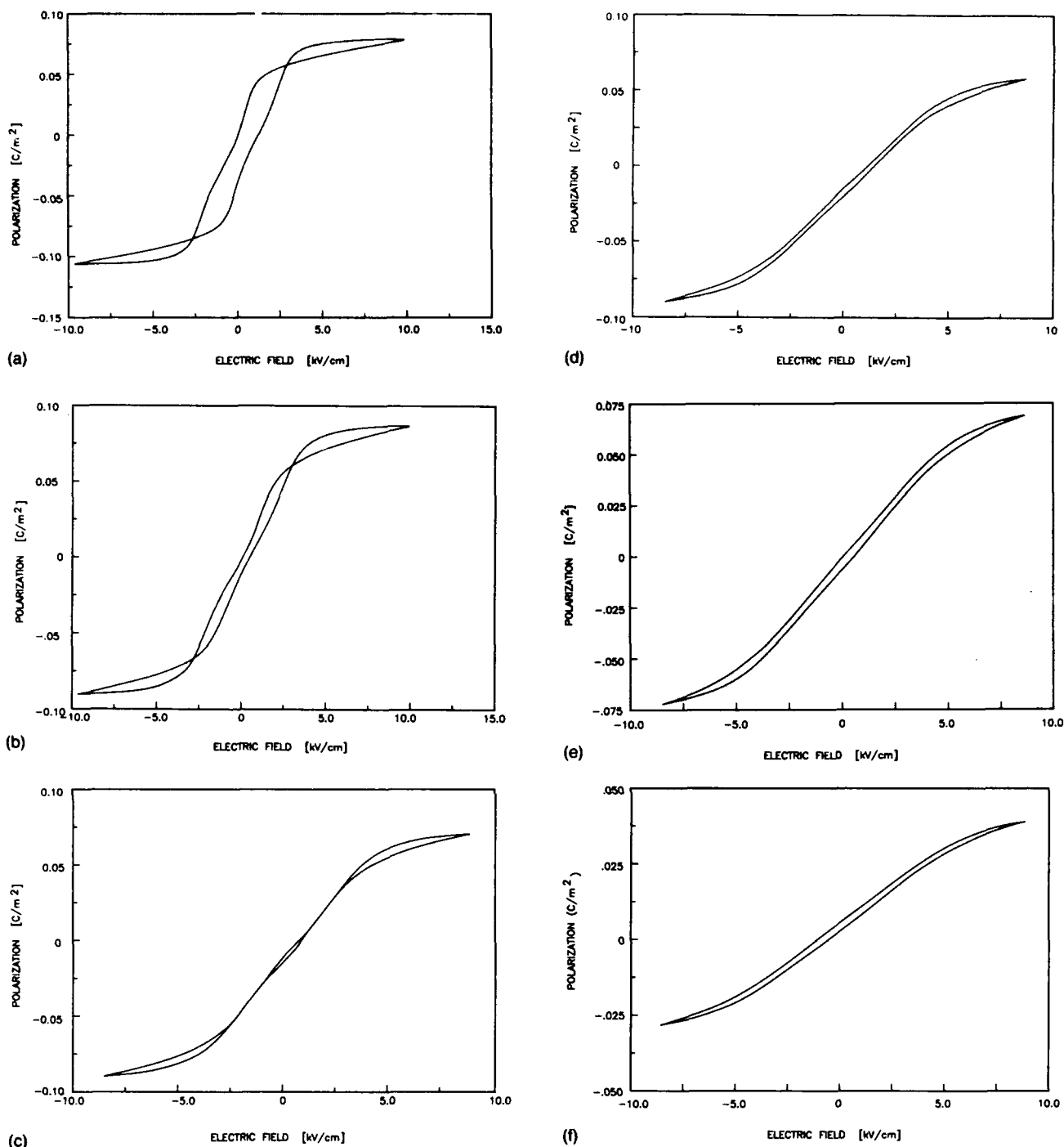


FIG. 7. Dielectric hysteresis of PMNPT-ST  $[0.975(0.859(\text{Pb}_3\text{MgNb}_2\text{O}_9)-0.141(\text{PbTiO}_3))-0.025 \text{ BaTiO}_3]$  at several temperatures. (a) 5 °C, (b) 15 °C, (c) 25 °C, (d) 35 °C, (e) 45 °C (f) 55 °C.

Fig. 4. The dielectric permittivity is calculated from the narrow hysteresis loops by averaging the two values of the dielectric displacement ( $+D$  and  $-D$ ) at each voltage level and then computing the piecewise slope of the resultant curve. The dielectric loss is estimated by adjusting the bridge to close the hysteresis loops and calculating the real and imaginary parts of the dielectric permittivity from the bridge parameters.

The mechanical displacement in the long lateral direction induced in the sample was measured simultaneously as

a function of electric field using a linear voltage differential transformer<sup>15</sup> (LVDT) as the field was varied between  $-10$  and  $10$  kV/cm. The samples were flat plates with approximate dimensions of  $5 \times 1.5 \times 0.43$  cm<sup>3</sup>. The output of the LVDT was connected to the y-axis input of the digital oscilloscope so that the mechanical displacement was read directly as a function of applied voltage. The data displayed on the oscilloscope was then entered directly into the computer for calculation of the strain versus field relationship.

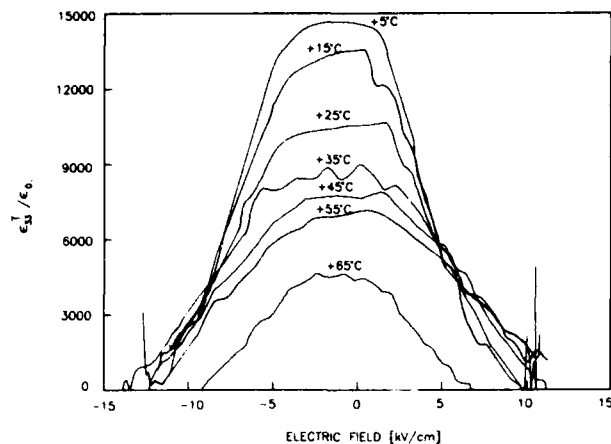


FIG. 8. Strong-field relative dielectric permittivity of PMNPT-ST [0.975(0.859(Pb<sub>3</sub>MgNb<sub>2</sub>O<sub>9</sub>)-0.141(PbTiO<sub>3</sub>))-0.025SrTiO<sub>3</sub>] as a function of electric field at various temperatures.

## II. RESULTS

### A. Measurements of dielectric properties

The weak-field dielectric constant and loss tangent are plotted in Figs. 5 and 6 for PMNPT-ST. The dielectric constant shows a broad maximum typical of the diffuse phase transition of ferroelectric relaxors. The peak in dielectric constant occurs at approximately 65 °C and is referred to as  $T_m$ . Below  $T_m$ , the thermal history influences the dielectric properties as evidenced by the different values on heating and cooling. The loss increases dramatically at low temperature. The knee in the weak-field dielectric loss occurs at about 50 °C. Pilgrim *et al.*<sup>15</sup> have suggested this temperature as the most logical definition for the transition temperature  $T_t$ . The weak-field dielectric properties of BT-doped PMNPT were virtually identical to those of the ST-doped material and are not shown.

The polarization of a PMNPT-ST sample is plotted as a function of electric field for various temperatures (Fig. 7). The relaxor ferroelectric nature of the materials is evident as the dielectric hysteresis observed at low temperature continually decays into just slightly lossy nonlinear behavior as the temperature increases.

The strong-field relative dielectric permittivity was calculated from the  $D$  vs  $E$  data at a frequency of 0.1 Hz. The nonlinear dielectric behavior is shown in Figs. 8 and 9, respectively, for PMNPT-ST and PMNPT-BT, at various temperatures. The strong-field dependence of the dielectric properties is obvious. The peak dielectric constants on the order of 18 000 should be observed near 20 °C. Higher dielectric constants were sometimes observed at lower temperatures. The exact location of the peak depends on the rate of cooling or heating and the thermal history of the sample. Heating and cooling the sample changes the observed peak in the strong-field dielectric properties as well as in the weak-field dielectric properties. The data are not reproducible below about 15 °C. This is an artifact of the thermal history of the material and not experimental error. It is also influenced by the presence of moisture near 0 °C.

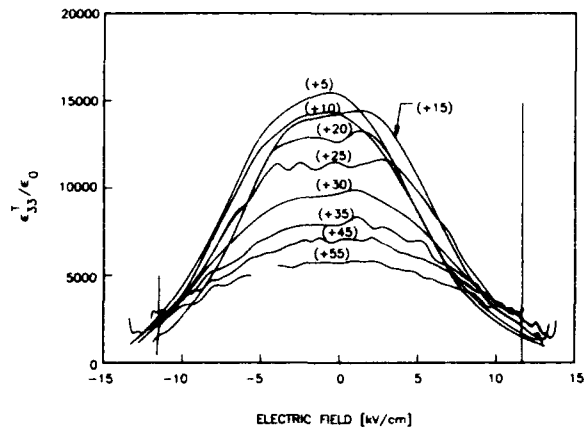


FIG. 9. Strong-field relative dielectric permittivity of PMNPT-BT [0.975(0.859(Pb<sub>3</sub>MgNb<sub>2</sub>O<sub>9</sub>)-0.025SrTiO<sub>3</sub>)] as a function of electric field at various temperatures.

### B. Direct measurement of piezoelectric properties

The values of  $(d_{33})_{\text{eff}}$  and  $(d_{31})_{\text{eff}}$  measured at 1 kHz for dc-bias fields of 1 and 2 kV/cm and are plotted in Figs. 10 and 11 for PMNPT-ST and in Figs. 12 and 13 for PMNPT-BT, respectively. All four plots show broad maximums near 20 °C with very slight thermal hysteresis. Only the real part of the piezoelectric coefficients were determined. At high temperatures, dielectric hysteresis is small enough to allow measurement of the materials at higher fields. The peak values of  $d_{33}$  and  $d_{31}$  for both PMNPT-ST and PMNPT-BT are approximately  $400 \times 10^{-12}$  and  $-190 \times 10^{-12}$  m/V under a dc-bias field of 2 kV/cm.

For PMNPT-ST  $(d_{33})_{\text{eff}}$  was measured as a function of applied bias field up to 7 kV/cm. The result is shown in Fig. 14 for 90 °C.

The elastic strain was measured as a function of the applied dc electric field. The strain hysteresis loops are plotted in Fig. 15 for PMNPT-ST at several different temperatures. At higher temperatures, the quadratic relationship at low electric field levels is apparent. At higher field levels, the strain starts to saturate. At temperatures below

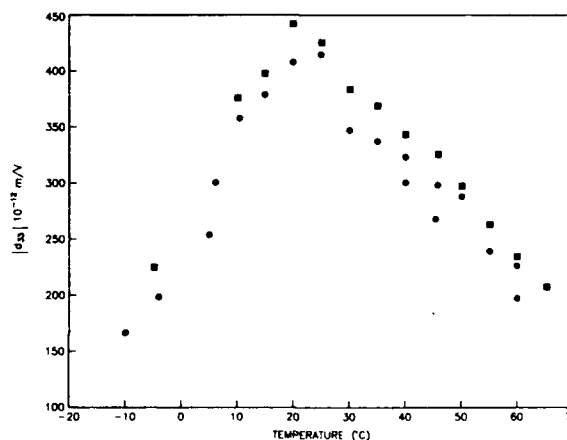


FIG. 10. Measured values of  $(d_{33})_{\text{eff}}$  for PMNPT-ST [0.975(0.859(Pb<sub>3</sub>MgNb<sub>2</sub>O<sub>9</sub>)-0.141(PbTiO<sub>3</sub>))-0.025SrTiO<sub>3</sub>] measured at 1 kHz as a function of temperature for dc bias of 2 kV/cm.

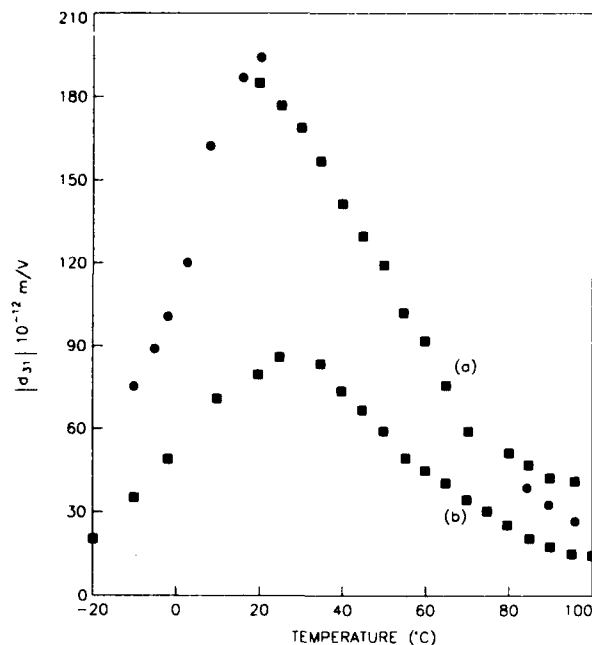


FIG. 11. Measured values of  $(d_{31})_{\text{eff}}$  for PMNPT-ST  $[0.975(0.859(\text{Pb}_3\text{MgNb}_2\text{O}_9)-0.141(\text{PbTiO}_3))-0.025 \text{ BaTiO}_3]$  measured at 1 kHz as a function of temperature for dc bias of (a) 2 kV/cm and (b) 1 kV/cm.

20 °C, the remanent polarization of the ceramic is switched at high-field levels causing hysteresis in the strain versus field relationship and eventually leads to the classic “butterfly” loops observed in ferroelectric materials well below the Curie temperature. The PMNPT-BT material showed excessive loss in the hysteresis measurements which would lead to dielectric breakdown.

### III. DISCUSSION

The low-field dielectric permittivity of both BT- and ST-doped PMNPT shows peaks near 60 °C. In contrast,

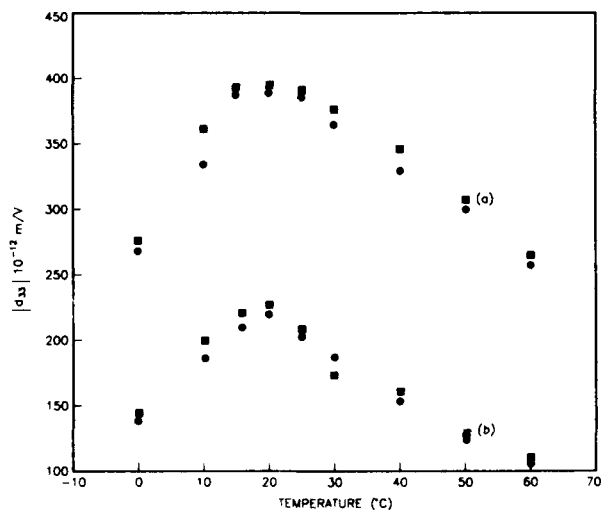


FIG. 12. Measured values of  $(d_{33})_{\text{eff}}$  for PMNPT-BT  $[0.975(0.859(\text{Pb}_3\text{MgNb}_2\text{O}_9)-0.141(\text{PbTiO}_3))-0.025 \text{ BaTiO}_3]$  measured at 1 kHz as a function of temperature for dc bias of (a) 2 kV/cm and (b) 1 kV/cm.

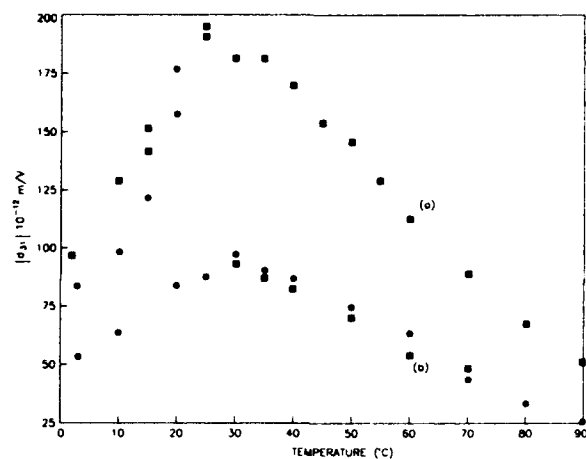


FIG. 13. Measured values of  $(d_{31})_{\text{eff}}$  for PMNPT-BT  $[0.975(0.859(\text{Pb}_3\text{MgNb}_2\text{O}_9)-0.141(\text{PbTiO}_3))-0.025 \text{ BaTiO}_3]$  measured at 1 kHz as a function of temperature for dc bias of (a) 2 kV/cm and (b) 1 kV/cm.

the peaks in the piezoelectric coefficients are observed near 25 °C. At high fields, the dielectric properties become increasingly less dependent on temperature. Near 4 kV/cm, the curves essentially merge together indicating that the temperature dependence is negligible. However, the dielectric constant at these fields is much lower. Hence, a trade-off between  $\epsilon_{33}^T$  and its temperature dependence is required. Clearly, the ionic mechanisms responsible for the dielectric and electromechanical relaxations are strongly dependent on the magnitude of electric field.

The peak in the measurement of the strong-field dielectric permittivity as a function of temperature occurs below 5 °C which is a lower temperature than where the peak in the piezoelectric constants occurs and far lower than the peak in weak-field dielectric permittivity. The location of the high-field peaks depend on the direction and rate of temperature change and on the frequency. The peak values of strong-field and weak-field dielectric permittivity differ because of this temporal dependence.

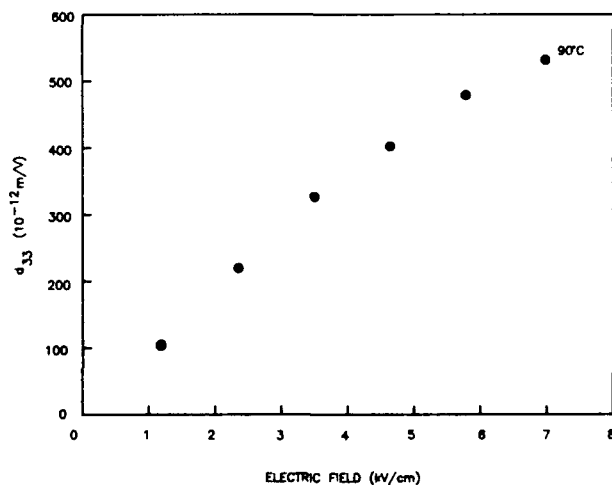


FIG. 14. Effective piezoelectric coefficient of PMNPT-ST  $d_{33}$  as a function of bias field at 90 °C.



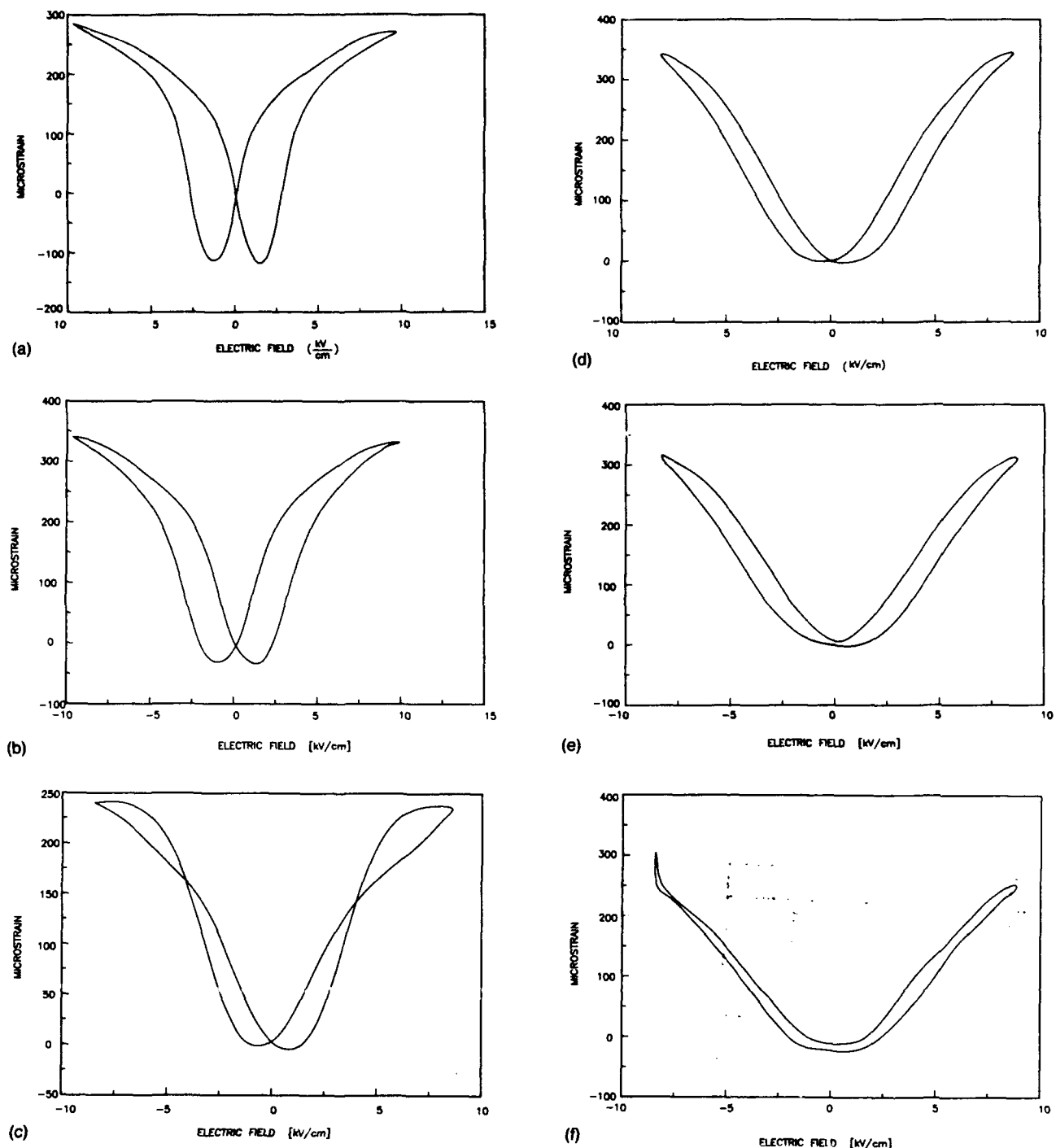


FIG. 15. Strain hysteresis for PMNPT-ST  $[0.975(0.859(\text{Pb}_3\text{MgNb}_2\text{O}_9)-0.141(\text{PbTiO}_3))-0.025\text{BaTiO}_3]$  at several temperatures (a) 5 °C (b) 15 °C (c) 25 °C (d) 35 °C (e) 45 °C (f) 55 °C.

The lowest temperature at which the material can be used is determined by the onset of the rapid increase in the strong-field dielectric loss and the increase in significant strain hysteresis. This, of course, depends on the intended application. For the compositions considered here, this rapid increase in loss occurs at 15–20 °C which is roughly in the middle of the operating range for underwater acoustic applications.

For practical application, the BT-doped PMNPT material showed excessive dielectric loss at electric fields of 2

kV/cm which led to thermal breakdown of the material at temperatures above 30 °C making the current formulation of the material unacceptable. The magnitude of the effective  $d_{33}$  coefficient over a range of temperature from 10–40 °C is similar in magnitude to conventional lead zirconate–titanate ceramics at very moderate dc-bias fields of 2.0 kV/cm. Large ac-fields can then be applied without causing excessive harmonic distortion. Higher dc-fields can undoubtedly be used, if desired, but will produce increasing nonlinearity. For many applications, the ceramic

should be dc-biased at the center of the region where the strain versus field relationship is linear. This will provide the highest nondistorted strain. High harmonic distortion decreases the output at the desired frequency. With the current experimental arrangement, measurements of piezoelectric properties at higher bias levels are unreliable at many temperatures due to dielectric breakdown. However, even at these field levels, the peak strains which can be produced are quite large. Other applications, could utilize the nonlinearity of the material to generate low frequency signals from the difference frequency of two high frequency signals using small, compact transducers.

#### IV. CONCLUSIONS

For practical application in underwater acoustics, the lower use temperature defined where the piezoelectric coefficients start to fall off, should be decreased 5–10 °C. It is questionable whether this could be accomplished with the PMNPT ceramics. Pure PMN will exhibit significant hysteresis at about –5 °C; however, as mentioned earlier, its dielectric constant and consequently, the maximum strain which can be generated is much smaller than the PMNPT ceramics. Alternatively, the transducer material could be heated and thermally stabilized in order to optimize its performance.

#### ACKNOWLEDGMENTS

The author would like to acknowledge Dr. Steve Pilgrim and the staff at Martin Marietta Laboratories, Baltimore, MD for preparing the samples used in this study under NRL Contract N00014-89-C-2357.

Accession For	
NTIS CRA&I	<input checked="" type="checkbox"/>
DTIC TAB	<input type="checkbox"/>
Unannounced	<input type="checkbox"/>
Justification .....	
By .....	
Distribution /	
Availability Codes	
Dist	Avail and/or Special
A-1	20

- <sup>1</sup> K. Uchino, "Electrostrictive actuators," *Cer. Bull.* **65**(4), 647–656 (1986).
- <sup>2</sup> K. Uchino, "Recent topics in ceramic actuators - to improve reliability and durability," *Proceedings of the 1990 IEEE 7th International Symp. of the Applications of Ferroelectrics* held at Urbana-Champaign, IL, June 1990 (IEEE, Piscataway, NJ).
- <sup>3</sup> L. E. Cross, "Relaxor ferroelectrics," *Ferroelectrics* **76**, 241–267 (1987).
- <sup>4</sup> R. Clark and J. C. Burfoot, "The diffuse phase transition in potassium strontium titanate," *Ferroelectrics* **8**, 505–506 (1974).
- <sup>5</sup> Q. Zhang, W. Pan, A. Bhalla, and L. E. Cross, "Electrostrictive and dielectric response in lead magnesium niobate-lead titanate (0.9 PMN-0.1 PT) and lead lanthanum zirconate titanate (PLZT 9.5/65/35) under variation of temperature and electric field," *J. Am. Cer. Soc.* **72**(4), 599–604 (1989).
- <sup>6</sup> S. Pilgrim, "Electromechanical properties of some  $\text{Pb}(\text{Mg}_{1/3}\text{Nb}_{2/3})\text{O}_3\text{-PbTiO}_3\text{-(Ba,Sr)TiO}_3$  ceramics: Part one," *J. Am. Cer. Soc.* (to be published).
- <sup>7</sup> S. L. Swartz and T. R. Shiout, "Fabrication of perovskite lead magnesium niobate," *Mater. Res. Bull.* **17**, 1245–1250 (1982).
- <sup>8</sup> Model 55L Laser Doppler vibrometer and associated optics and electronics, Dantec Corporation, Skovlunde, Denmark.
- <sup>9</sup> K. M. Rittenmyer and P. S. Dobbelday, "Determination of the temperature-dependent piezoelectric coefficients of piezoelectric composite materials," *J. Acoust. Soc. Am.* **91**, 2254–2260 (1992).
- <sup>10</sup> Model 610B, Trek Corp., Medina, NY.
- <sup>11</sup> Model 2300, Krohn-Hite Corp., Boston, MA.
- <sup>12</sup> Model 2300, Delta Design Inc., San Diego, CA.
- <sup>13</sup> W. Pan, E. Furman, G. O. Dayton, and L. E. Cross, "Dielectric aging effects in doped lead magnesium niobate: lead titanate relaxor ferroelectric ceramics," *J. Mater. Sci. Lett.* **5**, 647–649 (1986).
- <sup>14</sup> Fluorinert™ FC-43, 3M Corp., St. Paul, MN.
- <sup>15</sup> Model MHR100, Shaevitz Corp., Pennsauken, NJ.
- <sup>16</sup> S. Pilgrim, M. Massuda, and A. E. Sutherland, "Electromechanical determination of the high-field phase transition of  $\text{Pb}(\text{Mg}_{1/3}\text{Nb}_{2/3})\text{O}_3\text{-PbTiO}_3\text{-(Ba,Sr)TiO}_3$  relaxor ferroelectrics," *J. Am. Cer. Soc.* (to be published).